

25th International Meshing Roundtable

Frame Field Guided Topological Improvement for Hex Mesh using Sheet Operations

Rui Wang, Shuming Gao*, Zhihao Zheng, Jinming Chen

State Key Lab of CAD&CG, Zhejiang University, Hangzhou 310058, PR China

Abstract

High-quality hex meshes are crucial for finite element analysis. However, the quality of a hex mesh improved by geometric smoothing cannot guarantee to satisfy the requirement of finite element analysis. To this end, this paper puts forward an approach to topological optimization of hex mesh based on frame field and sheet operations, which improves the quality of the worst elements of the hex mesh by optimizing its topological structure. The approach first builds an initial frame field on the input hex mesh and optimizes it to obtain a high-quality frame field. Then, the problematic sheet that leads to the poor quality of the hex mesh is determined according to the initial and optimized frame fields. Finally, the structure of the problematic sheet is adjusted based on the high-quality frame field and sheet operations. Experimental results demonstrate that our topological optimization approach can effectively improve the minimal Scaled Jacobian value of the hex mesh.

© 2016 The Authors. Published by Elsevier Ltd.

Peer-review under responsibility of the organizing committee of IMR 25.

Keywords: hex mesh; mesh optimization; topological optimization; frame field; sheet operations.

1. Introduction

In finite element analysis, the quality of a hex mesh directly determines the precision and efficiency of simulation [1]. A poor quality element, such as a element with minimal Scaled Jacobian value less than 0.2, could make the mesh unusable for simulation. However, high-quality hex meshing is still an open problem, and mesh editing can easily lead to a degradation of the mesh quality, so to adequately support the subsequent numerical analysis, mesh optimization becomes essential.

Hex mesh improvement algorithms can be classified into two categories: geometric smoothing and topological optimization. Geometric smoothing [2], the most popular hex mesh improvement method, improves the overall quality of the hex mesh by optimizing the locations of mesh nodes. However, since geometric smoothing cannot change the topological connections between mesh nodes, the qualities of some hex meshes improved by geometric smoothing do not satisfy the analysis requirement.

* Corresponding author. Tel.: +86 571 88206681 ; fax: +86 571 88206680.

E-mail address: smgao@cad.zju.edu.cn

Unlike geometric smoothing, topological optimization allows to change the connections of mesh nodes during the optimization process, which can further improve the mesh quality after geometric smoothing. However, due to the global layered structure of hex mesh, efficient topological optimization of hex mesh becomes very difficult. Moreover, to date there are only several related works about hex mesh topological optimization [3,8–14].

In theory, there are three types of hex mesh topological modification operations [3]: flipping operation, atomic operation and sheet operation. Similar to the well-known flipping operations in tet meshes, Bern et al. [4] presented flipping operations for hex mesh, which translated several hexahedra into other hexahedra with the same boundary via several proposed patterns, and realized the localization of hex mesh modification. Tautges et al. [5] put forward a set of atomic operations that are irreducible by considering the mesh face as the object. Since the global structure of the hex mesh is not taken into account, these two kinds of topological modification operations are difficult to be applied to improve the mesh quality of hex mesh, so they are rarely used in hex mesh optimization. Sheet operations [6] regard the layered structure of a hex mesh (which is called sheet, or Spatial Twist Continuum [7]) as an operand. These operations change the topology of the hex mesh by the insertion and extraction of sheets, as well as adjusting the extension direction of sheets, and they are considered as the straightforward topological modification operation.

Sheet operation based hex mesh topological optimization can be divided into two categories, according to different optimization objectives: density optimization [8–10] and valence optimization [11–14]. The density optimization of hex mesh is carried out by means of adding or deleting elements to ensure the element densities are in line with requirements of the density function. Woodbury et al. [8] extracted the sheets locally by adding supplementary sheets to be able to coarsen the local region. Harris et al. [9] presented corresponding refinement templates for single and double sheet insertions, which could freely control the direction and region of mesh refinement. For the problem of uneven density of hex mesh after mesh editing, Zhu et al. [10] proposed the sheet operation based coarsening and refinement strategies to optimize the density of hex mesh. In addition, sheet operations can also be applied to optimize the valences of mesh edges to improve the mesh quality. Mitchell et al. [11] eliminated the doublet elements of hex mesh through Pillowing operation. Shepherd [12] and Qian et al. [13] used the Pillowing operation on the whole boundary of hex mesh generated by grid-based method to improve the mesh quality of the boundary elements. Ledoux et al. [14] converted a hex mesh into fundamental mesh by sheet operations, which improved not only the quality of boundary elements, but also the mesh elements associated to geometric surfaces or curves. On the whole, existing topological optimization algorithms can improve the mesh quality of hex mesh to different extents, but there lacks a targeted approach to improving the quality of the worst elements of the hex mesh.

Considering that the mesh elements with worst quality are the main reason for not being able to use the hex mesh for simulation, in this paper we present an approach of frame field guided topological improvement for hex mesh using sheet operations. Our focus is on improving the mesh quality of the worst elements in a hex mesh. The approach presented in this paper has the following main contributions:

- 1). We optimize the hex mesh under the guidance of a high-quality frame field, making its structure conform to the orientations of the frame field as far as possible, so as to improve its topological structure;
- 2). We regard the determined problematic sheet as the primary object of topological optimization, which can naturally reflect the relationships between topological structure of the hex mesh and the frame field and can guarantee the validity of the resultant mesh;
- 3). We present the approach of building a high-quality frame field on the hex mesh, which is able to guide the topological optimization for the hex mesh.

2. Basic Concepts and Approach Overview

Before describing the optimization approach, we introduce some basic concepts of dual structure of hex mesh and frame field. Due to a limited space, we omit some familiar concepts related to hex mesh, which are described elsewhere [15].

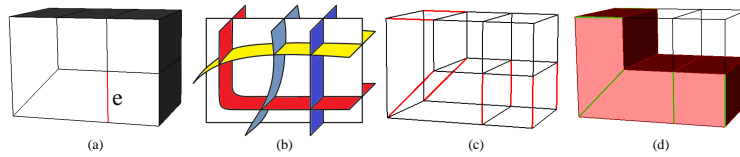


Fig. 1. Illustration of dual mesh: (a) a hex mesh and an edge e ; (b) the corresponding dual mesh with five sheets; (c)(d) another two representations of the sheet in red in (b).

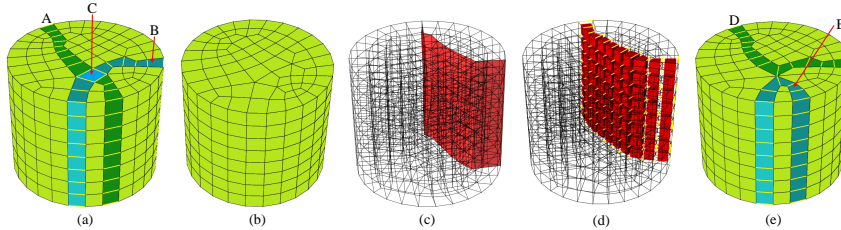


Fig. 2. Sheet operations: (a) sheets A and B, column C; (b) mesh after extracting sheet A; (c) a quad set; (d) the sheet inflating the quad set in (c); (e) mesh after collapsing column C.

2.1. Basic concepts

2.1.1. Dual mesh

Dual mesh is expressed as the topological structure of the finite element mesh in dual space, and it can be seen as a simple arrangement of 2D surfaces. Fig. 1(b) is the dual mesh of hex mesh in Fig. 1(a). There are certain relationships between the elements in a hex mesh, such as that the three groups of topological parallel mesh edges in each element. According to these parallel relationships, all the mesh edges in a hex mesh can be divided into different groups, and each group corresponds to a sheet in dual mesh.

Definition 1 (sheet). Given a hex mesh H and a mesh edge e in H , a sheet s can be represented as a set of edges E_s , where E_s is the maximum set of edges that can be recursively found by obtaining the topological parallel edges of e .

Similarly, the set of hex H_s that traverses through E_s , and the 2D surface which traverses the middle points of E_s , can also be seen as the sheet s . The red surface in Fig. 1(b), the edge group in red in Fig. 1(c) and the set of hex in Fig. 1(d) all represent the sheet corresponding to mesh edge e .

2.1.2. Sheet operation

The basic sheet operations [3,6] primarily include sheet extraction, sheet inflation and column collapse.

Sheet extraction [3,6] is a dual operation to delete the hexahedra of a sheet. For the sheet to be extracted, sheet extraction will degenerate the mesh edge of the sheet to a point and degenerate the hex of the sheet to a quad, as shown in Fig. 2(b). Sheet inflation [3,6] is a dual operation to generate a new sheet by inserting a layer of hexahedra, and this is the inverse operation of sheet extraction. In general, sheet inflation requires a quad set as the input (Fig. 2(c)), and generates the new sheet by inflating every quad in the quad set (the red sheet in Fig. 2(d)). Column collapse [3,6] can change the intersecting relationship between related sheets by removing the hexahedra in the column. As shown in Fig. 2(e), sheets A and B are turned into sheet D and E after collapsing column C.

2.1.3. Frame field

Frame field can offer the geometric orientations on the boundary and inside of the model, which is widely used in high-quality hex meshing [16–19]. In order to improve the quality of the hex mesh, we use frame field to guide the adjustment of the bad structure. Similar to [18,19], in this work the frame is defined as follows:

Definition 2 (frame). Given a 3-tuple of three unit 3D vectors $\mathbf{F} = \{\mathbf{u}, \mathbf{v}, \mathbf{w}\}$, if $\mathbf{u} \times \mathbf{v} \cdot \mathbf{w} = 1$, $\mathbf{u} \cdot \mathbf{v} = \mathbf{v} \cdot \mathbf{w} = \mathbf{w} \cdot \mathbf{u} = 0$, then \mathbf{F} is considered as a 3D frame.

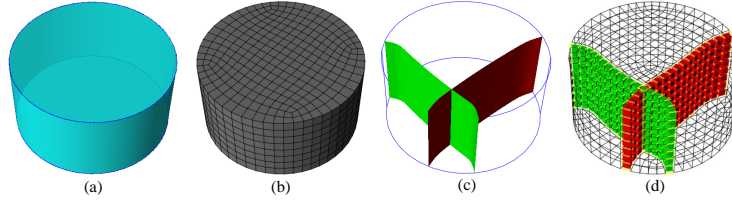


Fig. 3. The hex mesh generated based on frame field: (a) a solid model; (b) the generated hex mesh; (c) several iso-surfaces for 3D parameterization; (d) the corresponding sheets to iso-surfaces in (c).

In fact, frame can also be seen as a 3×3 orthogonal matrix $[\mathbf{u} | \mathbf{v} | \mathbf{w}]$, in which the column vectors are respectively three mutually perpendicular unit vectors in the frame. Frames \mathbf{F}_i and \mathbf{F}_j are considered equivalent if \mathbf{F}_i can be permuted to \mathbf{F}_j . There are 24 equivalent frames for each frame since the permutations form the chiral cubical symmetry group \mathcal{G} (any map in $SO(3)$ which maps coordinate axes to coordinate axes).

To be able to quantify the closeness between two frames, the matching matrix [18] is adopted, which is defined as follows:

Definition 3 (matching matrix). The matching matrix between frames \mathbf{F}_s and \mathbf{F}_t is defined as the best permutation between them:

$$\Pi_{st} := \operatorname{argmin}_{P \in \mathcal{G}} \left\| [\mathbf{u}_s | \mathbf{v}_s | \mathbf{w}_s] - [\mathbf{u}_t | \mathbf{v}_t | \mathbf{w}_t] P^T \right\|_F \quad (1)$$

where $\|\cdot\|_F$ is the Frobenius matrix norm.

The closeness of any two frames \mathbf{F}_s and \mathbf{F}_t [18] is approximated by the closeness between $\bar{\mathbf{P}}_{st} = [\mathbf{u}_t | \mathbf{v}_t | \mathbf{w}_t]^{-1} [\mathbf{u}_s | \mathbf{v}_s | \mathbf{w}_s]$ and \mathcal{G} :

$$E_{st} = \sum_i \left[H(\bar{\mathbf{P}}_{st}[\cdot, i]) + H(\bar{\mathbf{P}}_{st}[i, \cdot]) \right] \quad (2)$$

where $\bar{\mathbf{P}}_{st}[\cdot, i]$ and $\bar{\mathbf{P}}_{st}[i, \cdot]$ denote the i -th row and column vector of $\bar{\mathbf{P}}_{st}$ respectively, and $H(\eta) = \eta_x^2 \eta_y^2 + \eta_y^2 \eta_z^2 + \eta_z^2 \eta_x^2$.

Frame field based hex meshing mainly follows three steps: design a guiding frame field, generate a parameterization which aligns to the frame field and extract the hex mesh from the parameterization. By adopting this meshing method, we generate the hex mesh for the model in Fig. 3(a), which is of high quality. Fig. 3(c) illustrates several iso-surfaces for the 3D parameterization, and we can see clearly that the red iso-surface corresponds to the red sheet in Fig. 3(d), while the green iso-surface corresponds to the green sheet in Fig. 3(d). This is because the high-quality frame field contains the geometric information, and the parameterization is built to align with it hereafter, thus several extracted iso-surfaces can represent the ideal location and shape of the corresponding layer of hexahedra.

2.2. Overview of our approach

We now describe our topological improvement approach based on frame field and sheet operations, aiming to improve the mesh quality of the worst elements in the hex mesh. In this paper, the quality of each element of hex mesh is calculated by the minimal Scaled Jacobian value. The input of the approach are the hex mesh after geometric smoothing using the method in [20] and an acceptable minimal Scaled Jacobian value of the hex mesh defined by user, the hex mesh would still contain several elements that do not meet user's requirements. The output is the hex mesh whose minimal Scaled Jacobian value is improved.

In order to effectively utilize frame field to improve the worst quality of hex mesh through topological optimization, three critical problems need to be addressed: 1. How to automatically determine the poor topological structure which leads to the degradation of the mesh quality; 2. How to effectively adjust the poor topological structure to make the quality of the worst elements improved; and 3. How to establish a high-quality frame field on the input hex mesh. For the first problem, we determine the problematic sheet which degrades the quality of element by calculating the structural quality of all the related sheets and consider the problematic sheet as adjusting object. For the second problem, we adjust the structure of the problematic sheet based on the orientations offered by a high-quality frame field. For the third problem, we first build a frame on each hex according to its three main directions, and then minimize a global energy function to obtain a high-quality frame field.

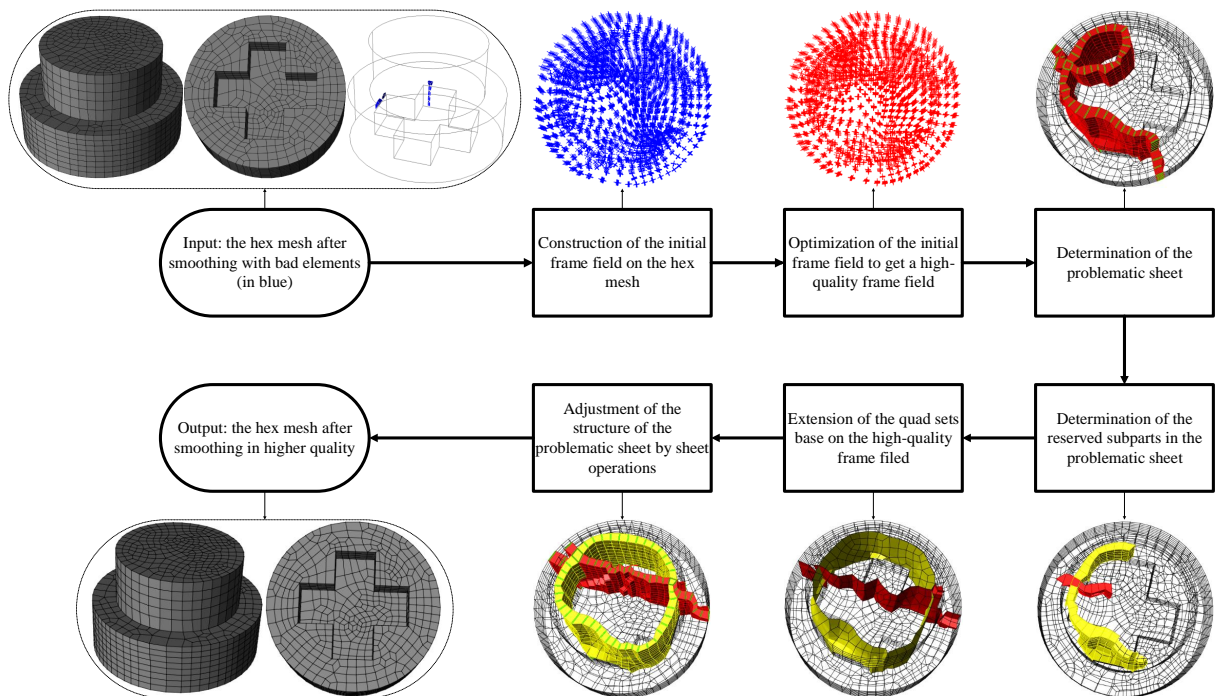


Fig. 4. The flowchart of frame field guided topological improvement for hex mesh using sheet operations.

As shown in Fig. 4, our approach consists of the following steps:

- 1). Build initial frame field on the input hex mesh and optimize it to obtain the high-quality frame field;
- 2). Determine the problematic sheet that degrades the mesh quality according to the initial and optimized frame fields;
- 3). Adjust the structure of the problematic sheet under the guidance of the high-quality frame field and the current structure of the hex mesh;
- 4). Do geometric smoothing on the hex mesh after topological optimization, and repeat the above steps until the mesh quality meets user's requirements or the worst quality cannot be further improved by our approach.

3. Construction of a high-quality frame field on hex mesh

A high-quality frame field of a solid model can reliably record the whole geometry information of boundary and inside of the model. Since it offers the orientations of the ideal hex mesh of the solid model, it can be used as the basis of topological optimization. We first build the initial frame field on the input hex mesh and then optimize it to get a high-quality frame field, enabling it to effectively guide the subsequent topological optimization.

3.1. Construction of the initial frame field on hex mesh

We first build a frame at the center of each hex, whose three vectors are three mutually perpendicular main directions of this hexahedron. In other words, each of the three vectors of the frame should be parallel to the three vectors linking the centers of three groups of topological parallel mesh faces in the hexahedron as far as possible. As shown in Fig. 5, \mathbf{X} , \mathbf{Y} , \mathbf{Z} are the three unit vectors separately linking the three groups of parallel mesh faces in a hexahedron. The initial frames are built individually according to the types of hexahedron: inner mesh hexahedra, boundary hexa-

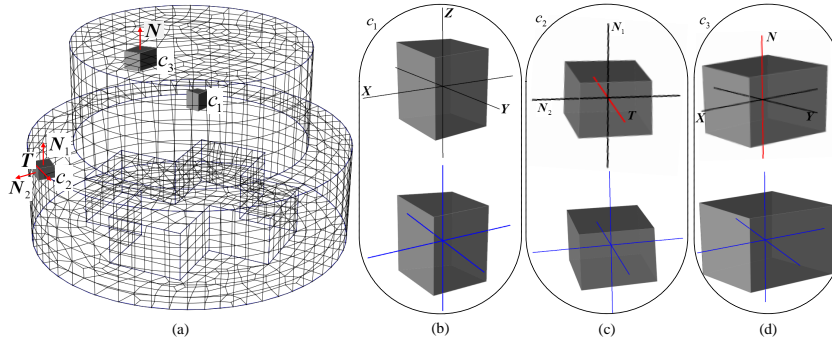


Fig. 5. The construction of the frame field on the hex mesh: (a) the hex mesh; (b)(c)(d) the construction of the frames on c_1 , c_2 and c_3 , respectively.

hedra associated to geometric curves and boundary hexahedra associated to geometric surfaces (which do not fall into the first two categories).

For the hexahedron inside the model, such as c_1 in Fig. 5(a), the frame is determined as follows:

$$\begin{aligned} \{\mathbf{u}, \mathbf{v}, \mathbf{w}\} &= \operatorname{argmin} \|\mathbf{u} - \mathbf{X}\|_2 + \|\mathbf{v} - \mathbf{Y}\|_2 + \|\mathbf{w} - \mathbf{Z}\|_2 \\ \text{s.t. } \mathbf{u} \cdot \mathbf{v} &= 0, \mathbf{v} \cdot \mathbf{w} = 0, \mathbf{w} \cdot \mathbf{u} = 0 \\ \|\mathbf{u}\|_2 &= \|\mathbf{v}\|_2 = \|\mathbf{w}\|_2 = 1 \end{aligned} \quad (3)$$

In order to naturally meet the orthogonal and unit constraints of \mathbf{u} , \mathbf{v} , \mathbf{w} , we adopt Euler angle to express the frame, i.e. $R_x(\alpha)R_y(\beta)R_z(\gamma)$, where α, β, γ are the Euler angles of the matrix $[\mathbf{u} | \mathbf{v} | \mathbf{w}]$. Therefore, an internal frame is converted into three degrees of freedom and Eq. 3 is equally converted into:

$$(\alpha, \beta, \gamma) = \operatorname{argmin}_{(\alpha, \beta, \gamma)} \|R_x(\alpha)R_y(\beta)R_z(\gamma) - [\mathbf{X} | \mathbf{Y} | \mathbf{Z}]\|_F \quad (4)$$

The frame in blue in Fig. 5(b) is the initial frame of c_1 .

For the purpose of boundary conforming of hex mesh, special treatment is considered on the boundary hexahedra.

For the boundary hexahedron associated to geometric curves that is at least adjacent to two geometric surfaces, such as c_2 in Fig. 5(a), one direction of the frame is fixed to the direction of tangent vector \mathbf{T} of the geometric curve, so the initial frame can be expressed as a form with a degree of freedom:

$$\{\cos(\theta)\mathbf{T}_1 + \sin(\theta)\mathbf{T}_2, -\sin(\theta)\mathbf{T}_1 + \cos(\theta)\mathbf{T}_2, \mathbf{T}\} \quad (5)$$

where \mathbf{T}_1 and \mathbf{T}_2 are two orthogonal unit vectors that are perpendicular to \mathbf{T} and θ can be calculated as follows:

$$\theta = \operatorname{argmin}_{\theta} \|\cos(\theta)\mathbf{T}_1 + \sin(\theta)\mathbf{T}_2 - \mathbf{N}_1\|_2 + \|-\sin(\theta)\mathbf{T}_1 + \cos(\theta)\mathbf{T}_2 - \mathbf{N}_2\|_2 \quad (6)$$

where \mathbf{N}_1 and \mathbf{N}_2 are the unit normal vectors of the adjacent geometric surfaces, as shown in Fig. 5(c).

Similarly, for the hexahedron that is adjacent to geometric surface, such as c_3 in Fig. 5(a), one direction of the frame should be the surface normal. The frame can also be expressed as the form with only one degree of freedom:

$$\{\cos(\theta)\mathbf{T}_1 + \sin(\theta)\mathbf{T}_2, -\sin(\theta)\mathbf{T}_1 + \cos(\theta)\mathbf{T}_2, \mathbf{N}\} \quad (7)$$

where \mathbf{T}_1 and \mathbf{T}_2 are two orthogonal unit vectors which are perpendicular to \mathbf{N} and θ can be calculated as follow:

$$\theta = \operatorname{argmin}_{\theta} \|\cos(\theta)\mathbf{T}_1 + \sin(\theta)\mathbf{T}_2 - \mathbf{X}\|_2 + \|-\sin(\theta)\mathbf{T}_1 + \cos(\theta)\mathbf{T}_2 - \mathbf{Y}\|_2 \quad (8)$$

where \mathbf{X} and \mathbf{Y} are the two vectors which are perpendicular to \mathbf{N} as far as possible among the three vectors $\mathbf{X}, \mathbf{Y}, \mathbf{Z}$, as shown in Fig. 5(d).

The initial frame field is built on the hex mesh according to the above method. Unlike the previous methods whose frames are built on tet meshes, the frame field built on hex mesh in this way can naturally reflect the topological structure and the whole directional information of the current hex mesh, and subsequent optimization can also converge faster due to the higher quality of the initial frame field. Fig. 6(b) shows the initial frames of the sheet in Fig. 6(a). We observe that one direction (in red) of every frame is vertical to the 2D surface of this sheet, properly reflecting the direction of the sheet in the initial hex mesh, which is the important basis to evaluate the structural quality of a sheet.

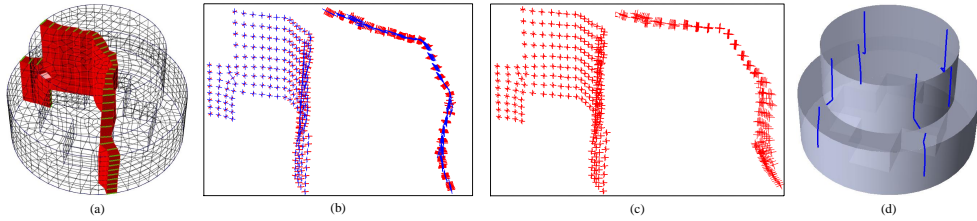


Fig. 6. The frames in a sheet: (a) a sheet in red; (b) two perspectives of the initial frames in the sheet; (c) the same perspectives with (b) of the frames after optimization in the sheet; (d) the extracted singularity edges.

3.2. Frame field optimization on hex mesh

After establishing the initial frame field, we optimize it to get a high-quality frame field (similar to [18]). The closeness E_{st} between the frames \mathbf{F}_s and \mathbf{F}_t is computed as shown in Eq. 2, and so the energy function for the whole field is defined as:

$$E = \sum_{f \in F_{inner}} E_f \quad (9)$$

where F_{inner} is the set of the inner mesh faces of hex mesh and E_f denotes the closeness E_{st} of frames on the two hexahedra (s and t) which are adjacent to mesh face f .

In frame field optimization, the inner frames are expressed as $R_x(\alpha)R_y(\beta)R_z(\gamma)$, whereas the boundary frames are expressed as $\{\cos(\theta)\mathbf{T}_1 + \sin(\theta)\mathbf{T}_2, -\sin(\theta)\mathbf{T}_1 + \cos(\theta)\mathbf{T}_2, \mathbf{T}(\mathbf{N})\}$. We use the L-BFGS method to achieve the minimal value. Since the energy function is non-linear, building the initial frame field in this way provides a better initial value for optimization, which avoids for the optimization to fall into local optimal solutions to some extent and also accelerates the convergence. Fig. 6(d) displays the extracted singular edges after frame field optimization.

The initial frame field expresses the topological structure of the input hex mesh, whereas the high-quality frame field after optimization offers the ideal topological structure of the hex mesh in the solid model. This comparison can clearly determine the bad topological structure of the input hex which do not conform to the best orientations, which is an important basis of our topological improvement. This information cannot be obtained from the frame field built on tet meshes. Fig. 6(c) shows the high-quality frames of the sheet in Fig. 6(a), some of which have dramatic improvements compared to the initial frames in Fig. 6(b).

4. Determination of the problematic sheet

If the hex mesh improved by geometric smoothing has remaining elements with poor quality, then there are some problems with the topological structure of the surrounding area of these elements. Since the topology of the hex mesh is formed by the intersection of a number of sheets, the structures of several sheets around these bad elements may be problematic. Based on this observation, the sheets which go through the bad elements and have poor structure qualities form the main topological structure that degrade the mesh quality. We refer to the sheet with the poorest structural quality as the problematic sheet, which should be determined first.

We consider all the sheets that go through the elements in poor quality as candidate sheets, and then determine the problematic sheet among them according to the structural qualities of sheets. Since the three directions of initial frame can express the directions of the three sheets that pass through the corresponding hexahedron, whereas the three directions of the high-quality frame after optimizing the initial frame express the ideal way of three sheets passing through the same hexahedron (i.e. the three 2D surfaces respectively normal to the three vectors of the frame), we can finally define the structural quality of a sheet s by the differences between the initial frame and the high-quality frame on the sheet:

$$D_s = \sum_{c \in H_s} \lambda_c E_{f_c \bar{f}_c} \quad (10)$$

where H_s is the set of hex in s , f_c is the initial frame on element c in H_s , \bar{f}_c is the high-quality frame on c , $E_{f_c \bar{f}_c}$ is the closeness between f_c and \bar{f}_c , λ_c is the weight of each hexahedron ($\lambda_c = 1/(t_c + 1)$, t_c is the topological distance from element c to the worse elements). The larger D_s is, the worse the structural quality of sheet s is.

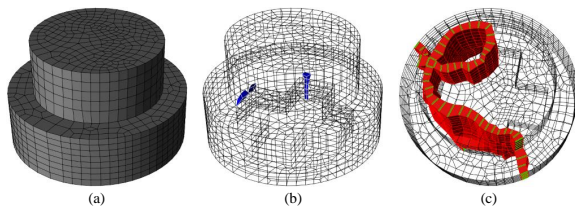


Fig. 7. The determination of the problematic sheet: (a) the hex mesh; (b) the 7 elements in poor quality; (c) the determined problematic sheet.

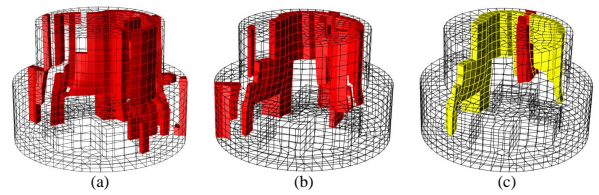


Fig. 8. The determination of the reserved subparts: (a) the initial reserved subparts; (b) the reserved subparts after optimization; (c) the determined reserved subparts in high proportion.

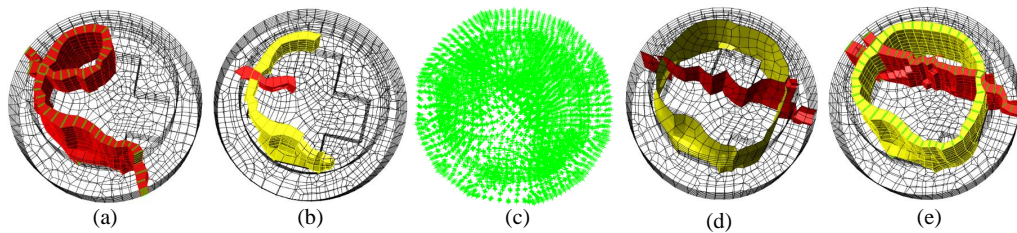


Fig. 9. The adjustment of the problematic sheet: (a) the problematic sheet; (b) the reserved subparts of sheet; (c) the frame field built on mesh faces; (d) the extended quad sets based on the frame field in (c); (e) the adjusted sheets of the problematic sheet in (a).

The problematic sheet is determined as the sheet with the maximum structural quality among candidate sheets. Fig. 7(b) illustrates the hexahedra in poor quality after smoothing (the mesh quality of these elements do not conform to user's requirement), and the determined problematic sheet is shown in red in Fig. 7(c).

5. Frame field guided topological adjustment using sheet operations

Since the high-quality frame field provides the information of the ideal arrangement of sheets, we adjust the structure of the problematic sheet resulting in poor quality to optimize the topological structure around these bad elements, so as to improve the mesh quality of the elements. Firstly, we determine the reserved subparts in the problematic sheet, i.e. the fixed region in process of topological modification, as shown in Fig. 9(b). Secondly, we build face frame field based on the high-quality frame field on the hex mesh, as shown in Fig. 9(c). Thirdly, by considering the one side of quads of each reserved subpart as a base quad set, we extend it to get the ideal quad set for inflation driven by the previous face frame field. Fig. 9(d) shows the extended quad sets for the two reserved subparts, respectively. Finally, we use the combined operations of local sheet extraction and local sheet inflation to adjust the structure of the problematic sheet. Fig. 9(e) shows the final adjusted sheets for the sheet initially shown in Fig. 9(a).

5.1. Determination of the reserved subparts in the problematic sheet

During sheet adjustment, several reserved subparts in the problematic sheet will be remained in order to keep the reasonable parts of the original sheet, whereas the other subparts of the sheet will be extracted. The reserved subparts consist of high-quality subparts and some other subparts. And the high-quality subparts are determined according to the following two rules:

1. The mesh quality of the hexahedra in the high-quality subparts is good;
2. The differences between the initial frame and the optimized high-quality frame on the hexahedra in the high-quality subparts are not big.

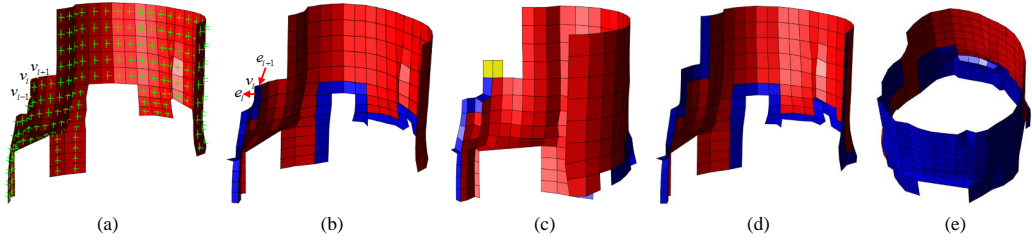


Fig. 10. The illustration of extension of the quad set based on frame field: (a) the base quads Q ; (b) the quad set Q after adding some quads (in blue); (c) the determination of the quads at v_i ; (d) the quad set Q after adding one layer of the quads (in blue); (e) the whole extended quad set.

Besides the high-quality subparts, in order to ensure that the quality of the hex mesh will not get worse during the sheet adjustment, the subparts of the sheet whose extraction will lead the topological quality of the resultant mesh worse are also remained. We determine these subparts by predicting the topological quality of the hex mesh after sheet extraction [21].

In this way, all reserved subparts are determined. Fig. 8(a) illustrates the initial reserved subparts of sheet in Fig. 9(a). To facilitate the sequence structure adjustment, we need to do simple optimization on the initial subparts, i.e. by removing hanging hex and adding several hex in little holes. The optimized reserved subparts are shown in Fig. 8(b). The reserved subparts are then divided into several connected regions and the regions with few hexahedra (where the hex number is less than 15% of the hex number of the corresponding sheet) are ignored so as to keep the mesh density of the mesh since each connected region denotes a potential new adjusted sheet. The reserved subparts whose extraction will lead the quality worse are always remained during the above optimization. The self-intersected sheet is considered as two sheets in the local. Fig. 8(c) illustrates the final two reserved subparts.

5.2. Construction of the face frame field on hex mesh

In the hex mesh, the location of the sheet can be determined by its quad set. The process of adjusting the sheet is the process of determining an ideal quad set for inflation, therefore to determine the ideal quad set more effectively, we establish the face frame field on the mesh faces of hex mesh.

For the inner mesh face f , the frame can also be expressed by Euler angle, $R_x(\alpha)R_y(\beta)R_z(\gamma)$, and its frame is defined as the mean frame of the two frames on the adjacent hexahedra:

$$(\alpha, \beta, \gamma) = \underset{(\alpha, \beta, \gamma)}{\operatorname{argmin}} \left(\left\| R_x(\alpha)R_y(\beta)R_z(\gamma) - [\mathbf{F}_s] \right\|_F + \left\| R_x(\alpha)R_y(\beta)R_z(\gamma) - [\mathbf{F}_t] \right\|_F \right) \quad (11)$$

where s and t are the two hexahedra adjacent to f , \mathbf{F}_s and \mathbf{F}_t are the frames on s and t .

5.3. Face frame field driven quad set extension

After establishing the frame field on mesh faces of hex mesh, for each reserved subpart, we consider its one side of quads as the base quad set and extend it to a valid quad set for inflation, based on the guiding of face frame field and the current topological structure of the hex mesh. Each extended quad set denotes a new adjusted sheet. One of the base quad sets and the frames are shown in Fig. 10(a).

We determine the final quad set by way of expanding outward, layer by layer. Assuming the outer boundary of the current base quad set Q is $l_0 = \{v_0, v_1, \dots, v_i, \dots, v_{l_0}\}$, in which $\{v_i\}$ is the ordered mesh vertices on l_0 . Each vertex v_i is handled in order, the two adjacent mesh edges of v_i on the boundary of quad set Q are e_i and e_{i+1} , as shown in Fig. 10(b). We need to determine a group of continuous mesh faces from edge e_i to e_{i+1} to be put into quad set Q . Because there may be more than one group of mesh faces from e_i to e_{i+1} , we finally select the one with best quality. The quality of each group G of mesh faces is computed as below:

$$E_G = E_{frame} (1 + E_{topology}) \quad (12)$$

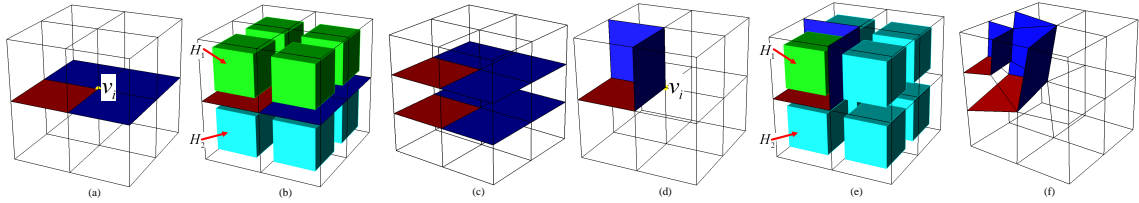


Fig. 11. Different impacts on the mesh quality of different quad sets G : (a) the base quad set (in red) and one group of quad set (in blue) around v_i ; (b) the hex set adjacent to v_i is separated into H_1 and H_2 by the quads in (a); (c) mesh edges on quads in (a) are split after sheet inflation; (d) the base quad set (in red) and another group of quad set (in blue) around v_i ; (e) the hex set adjacent to v_i is separated into H_1 and H_2 by the quads in (d); (f) mesh edges on quads in (d) are split after sheet inflation.

where E_{frame} is the sum of the differences between frames of faces in base quad set Q and the candidate group G , $E_{topology}$ is the impact of topological quality after adding the quads of G into base quad set Q . The larger E_G is, the lower chance for the group to be selected. A detailed description for each criterion is listed as below.

Frame field offers ideal orientations of sheet in hex mesh, which is the important basis to determine the quad set:

$$E_{frame} = \sum_{f \in G} \sum_{f_i \in N(f) \cap Q} E_{F_f F_{f_i}} \quad (13)$$

where $N(f)$ is the set of mesh faces which are adjacent to mesh face f , $E_{F_f F_{f_i}}$ is the closeness of frames on mesh faces f and f_i .

Considering that a valid quad set cannot be always identified based on the frame field alone, especially when the optimized frame field do not correspond to a reasonable structure of the hex mesh, we take into account the impact of topological quality after inflating the quad set during the process of determining the quad set:

$$E_{topology} = (\#H_1 - \#H_2)^2 \quad (14)$$

After adding G into Q , the set of hexahedra around vertex v_i is separated into two parts H_1 and H_2 . The closer $\#H_1$ (the number of hexahedra in H_1) is to $\#H_2$ (the number of hexahedra in H_2), the higher topological quality is after the inflation of the quad set. As shown in Fig.11, the topological quality of the resultant mesh is higher by selecting the quad set (in blue) in Fig. 11(a) compared to the quad set (in blue) in Fig. 11(d).

In this way, we can determine a group of continuous mesh faces from e_i to e_{i+1} , and then push these quads into the quad set Q . The quads in yellow in Fig. 10(c) are the determined mesh faces from e_i to e_{i+1} . After updating the quad set Q , we continue to handle the next mesh vertex v_{i+1} . The original quad set will be expanded a layer of quads after all the vertices on l_0 are processed, as shown in Fig. 10(d). After that we need to again identify the boundary vertices of the updating quad set Q , and to continue expanding the quad set until Q reaches the boundary of model or Q is self-enclosed. Finally, a valid quad set is determined in the end, as the quad set shown in Fig. 10(e).

In our specific implementation, we optimize the intermediate quad set after expanding each layer of quads, so as to guarantee that the expanding process will be convergent as much as possible.

After generating the quad set for each reserved subpart, we adjust the structure of the problematic sheet using sheet operations. We first do local sheet extraction on the problematic sheet, i.e. fixing the reserved subparts and degenerating other hex into quads. As shown in Fig. 12(b), several prisms will be formed in the process. We then perform local sheet inflation on the resultant hex mesh, i.e. inflating the quads (such as the blue quads in Fig. 10(e)), but only those that are in the determined quad set and not in the initial base quad set. Using this method, the structure of the problematic sheet is effectively optimized. Fig. 12(c) shows the new adjusted sheets for the problematic sheet in Fig. 12(a).

6. Experimental results

The proposed approach is implemented using the C++ programming language on an Intel i7-4790 CPU with 8GB of RAM. The approach has been tested on different meshes after mesh cutting, mesh matching and mesh morphing. The acceptable minimal Scaled Jacobian value is input by the user (it is set to 0.3 in Test cases 1, 2, 3 and 4, and is set to 0.4 in Test case 5). The statistics of quality (including Scaled Jacobian, Hex Shape and Hex Skew [22]) of the

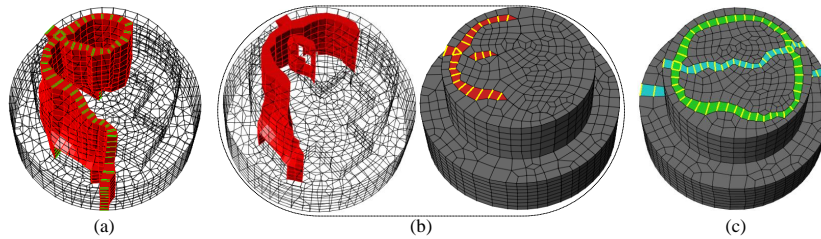


Fig. 12. The adjustment of the problematic sheet: (a) the original hex mesh with the problematic sheet; (b) the intermediate mesh after local sheet extraction; (c) the final hex mesh after inflating the new quad sets.

Table 1. The quality statistics and the running times.

	Hex Num.		Scaled Jacobian (Mean\Min)		Hex Shape (Mean\Max)		Hex Skew (Mean\Min)		Running Time(s)	
	Initial	Final	Initial	Final	Initial	Final	Initial	Final	Frame Opt.	Sheet Adjust
Test Case 1	4007	4208	.871\0	.880\,359	.891\0	.892\,538	.950\0	.955\,640	99.5	21.5
Test Case 2	7088	7264	.943\-.054	.941\,341	.962\,321	.960\,625	.982\,514	.982\,807	231.9	5.8
Test Case 3	9592	10222	.927\,196	.930\,332	.949\,480	.946\,570	.975\,572	.977\,733	258.2	22.8
Test Case 4	5149	5117	.941\-.009	.946\,538	.964\0	.969\,680	.979\0	.983\,736	100.7	1.5
Test Case 5	4880	4792	.913\,355	.929\,445	.943\,622	.954\,660	.969\,664	.976\,744	67.9	10.6

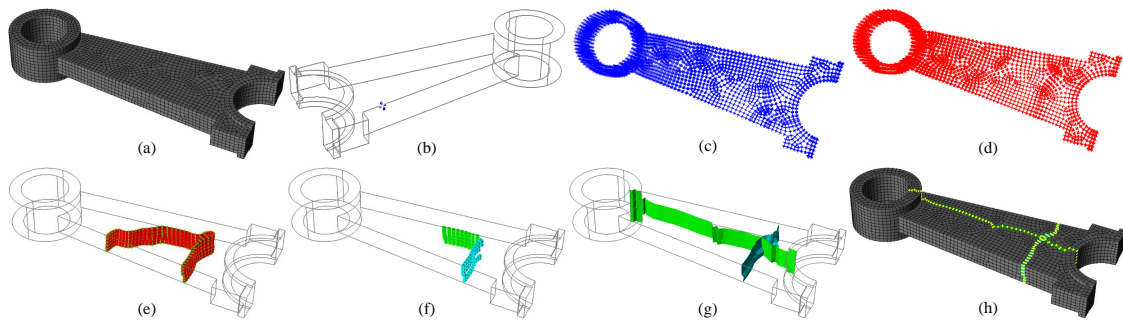


Fig. 13. The major processes of topological improvement for Test case 2: (a) the input hex mesh; (b) the bad elements that do not meet user's requirement (in blue); (c) the initial frame field; (d) the high-quality frame field; (e) the problematic sheet; (f) the reserved subparts; (g) the determined quad sets; (h) the mesh after adjusting the structure of the problematic sheet.

input meshes (after geometric smoothing) and the output meshes, as well as the timings spent on the initialization and optimization of the frame field (Frame Opt.) and the determination and adjustment of the problematic sheet (Sheet Adjust) are respectively given in Table 1.

The hex mesh shown in Fig. 13(a) is an intermediate mesh during mesh matching. After smoothing, the minimal Scaled Jacobian of the mesh is -0.054 , which is unacceptable. The minimal Scaled Jacobian of the hex mesh after topological improvement is increased to 0.341 . The hex mesh in Fig. 14 is the resultant mesh after mesh morphing (moving the feature F in Fig. 14(a)). In the optimization process, two reserved subparts are identified, so two sheets are inserted instead of the initial problematic sheet. The minimal Scaled Jacobian value of the mesh is increased to 0.332 . However, as shown in Fig. 14(e), the quad set in green is extended from the base quad set from subpart in green in Fig. 14(d), leading the sheet structure to be altered very much, which in turn changes the initial mesh density to a certain extent. Reducing this effect will be our focus in future work.

Test case 4 shown in Fig. 15(a) has several elements whose quality do not satisfy the user's requirement. The extracted singularity edges of the high-quality frame field of the model are shown in Fig. 15(c), which demonstrates the optimized frame field is optimal for this model. After adjusting the structure of the problematic sheet (Fig. 15(d)), the minimal Scaled Jacobian of the hex mesh is increased to 0.538 . However, since the optimization problem defined in Eq. 9 is non-linear, not all frame fields can be optimized to be very good. For example, the optimized frame field of the hex mesh in Fig. 16(a) is not good, which can be seen from the extracted singularity edges in Fig. 16(c), and thus the problematic sheet in Fig. 16(d) is hard to be well adjusted only based on this frame field. In our approach, since the topological structure of the initial hex mesh is also used to guide the adjustment of the problematic sheet (Sec. 5.3), so the minimal Scaled Jacobian of the hex mesh in Fig. 16(a) is still improved to 0.445 .

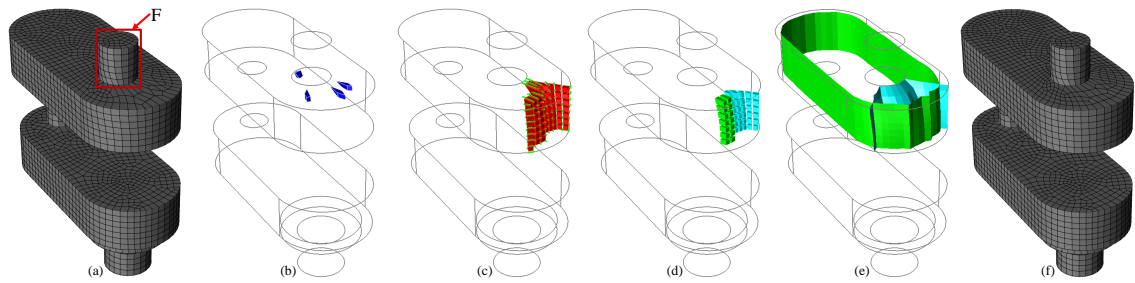


Fig. 14. The major processes of topological improvement for Test case 3: (a) the input hex mesh; (b) the bad elements (in blue); (c) the problematic sheet; (d) the reserved subparts; (e) the determined quad sets; (f) the resultant mesh.

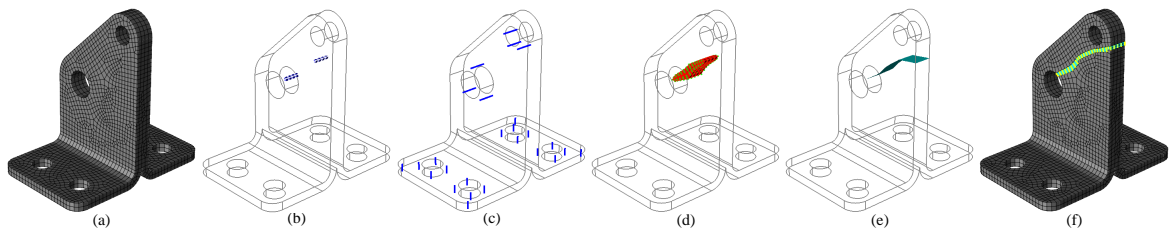


Fig. 15. The major processes of topological improvement for Test case 4: (a) the input hex mesh; (b) the bad elements (in blue); (c) the extracted singularity edges of the high-quality frame field; (d) the problematic sheet; (e) the determined quad set; (f) the resultant mesh.

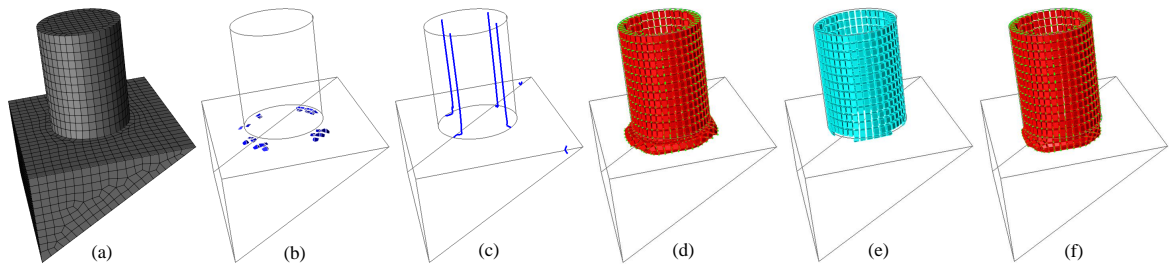


Fig. 16. Several processes of topological improvement for Test case 5: (a) the input hex mesh; (b) the bad elements (in blue); (c) the extracted singularity edges of the high-quality frame field; (d) the problematic sheet; (e) the reserved subpart; (f) the adjusted sheet of the sheet in (d).

In addition, as listed in Table 1, the optimization of the frame field costs a lot of time currently. We think that it is due to our current poor implementation of the optimization solving and can be dramatically improved in the near future according to [18].

7. Conclusion and future work

This paper presents a novel approach to topological optimization of the hex mesh, focusing on improving the quality of the worst elements. The proposed approach has the following advantages compared with existing methods:

- 1). By converting the worst quality problem into the structure problem of the related sheets, the approach can effectively improve the quality of the worst elements by optimizing the sheet structure via sheet operations.
- 2). By establishing the initial and optimized frame fields of the input hex mesh, we can effectively find the problematic sheet and optimize its structure under the guidance of the optimized frame field and the current structure of the hex mesh.

Several improvements of our approach are planned in our future work:

- 1). In our current approach, we adopt local measures to determine the quad set guided by frame field, and sometimes the determined quad set may not be the optimal one and the validity of the quad set cannot be guaranteed for complex models. Therefore, in the future, we will build the parameterization aligning to the high-quality frame field, and we will get the ideal quad sets by directly extracting the iso-surfaces. In addition, more complex mesh models will be tested in the future.
- 2). We will also consider the impact of the mesh density during the optimization process in the future so as to keep the initial mesh density as far as possible. Besides, other quality measures such as mesh density and mesh topological quality will be also taken into account to be able to better determine the problematic structure.

Acknowledgements

The authors are very grateful to the financial supports from NSF of China (61572432) and National 863 High Technology Plan (2013AA041301).

References

- [1] T. Blacker, Automated conformal hexahedral meshing constraints, challenges and opportunities, *J. Engineering with Computers*, 17.3 (2001) 201–210.
- [2] P. M. Knupp, Achieving finite element mesh quality via optimization of the Jacobian matrix norm and associated quantities. Part II-A framework for volume mesh optimization and the condition number of the Jacobian matrix, *J. International Journal for Numerical Methods in Engineering*, 48.8 (2000) 1165–1185.
- [3] F. Ledoux, J. Shepherd, Topological Modifications of Hexahedral Meshes via Sheet Operations: a Theoretical Study, *J. Engineering with Computers*, 26(2010) 433–447.
- [4] M. Bern, D. Eppstein, J. Erickson, Flipping Cubical Meshes, *J. Engineering with Computers*, 18.3(2002) 173–187.
- [5] T. J. Tautges, S. E. Knopp, Topology Modification of Hexahedral Meshes using Atomic Dual-based Operations, in: *Proceedings of the 12th International Meshing Roundtable*, 2003, 415–423.
- [6] M. L. Staten, J. F. Shepherd, F. Ledoux, K. Shimada, Hexahedral Mesh Matching: Converting non-conforming hexahedral-to-hexahedral interfaces into conforming interfaces, *J. International Journal for Numerical Methods in Engineering*, 82.12 (2010) 1475–1509.
- [7] P. Murdoch, S. Benzley, T. Blacker, et al, The Spatial Twist Continuum: A Connectivity Based Method for Representing All-hexahedral Finite Element Meshes, *J. Finite Elements in Analysis and Design*, 28.2(1997) 137–149.
- [8] A. C. Woodbury, J. F. Shepherd, M. L. Staten, et al. Localized Coarsening of Conforming All-hexahedral Meshes, *J. Engineering with Computers*, 27.1(2011) 95–104.
- [9] N. J. Harris, S. E. Benzley, S. J. Owen. Conformal Refinement of All-Hexahedral Element Meshes Based on Multiple Twist Plane Insertion, in: *Proceedings of the 13th International Meshing Roundtable*, 2004, 157–168.
- [10] H. Zhu, J. Chen, H. Wu, S. Gao. Direct Editing on Hexahedral Mesh through Dual Operations, *J. Procedia Engineering*, 2014, 149–161.
- [11] S. A. Mitchell, T. J. Tautges. Pillowing Doublets: Refining a mesh to ensure that faces share at most one Edge, in: *Proceedings of the 4th International Meshing Roundtable*, 1995, 231–240.
- [12] J. F. Shepherd. Conforming Hexahedral Mesh Generation via Geometric Capture Methods, in: *Proceedings of the 18th International Meshing Roundtable*, 2009, 85–102.
- [13] J. Qian, Y. Zhang, Automatic Unstructured All-hexahedral Mesh Generation from B-Reps for Non-manifold CAD Assemblies, *J. Engineering with Computers*, 28.4 (2012) 345–359.
- [14] F. Ledoux, Le Goff N, S. J. Owen, et al. A Constraint-Based System to Ensure the Preservation of Sharp Geometric Features in Hexahedral Meshes, in: *Proceedings of the 21st International Meshing Roundtable*, 2013, 315–332.
- [15] F. Ledoux, J. Shepherd, Topological and geometrical properties of hexahedral meshes, *J. Engineering with Computers*, 26.4 (2010) 419–432.
- [16] M. Nieser, U. Reitebuch, K. Polthier, Cubecover-parameterization of 3d volumes, in: *Computer Graphics Forum*, 2011, pp. 1397–1406.
- [17] J. Huang, Y. Tong, H. Wei, et al. Boundary aligned smooth 3D cross-frame field, *J. ACM Transactions on Graphics*, 2012, 30.6 (2012) 61–64.
- [18] Y. Li, Y. Liu, W. Xu, et al. All-hex meshing using singularity-restricted field, *J. ACM Transactions on Graphics*, 31.6 (2012) 439–445.
- [19] N. Kowalski, F. Ledoux, P. Frey, Block-structured hexahedral meshes for CAD models using 3D frame fields, *J. Procedia Engineering*, 82 (2014) 59–71.
- [20] E. Ruiz-Girons, X. Roca, J. Sarrate, et al. Simultaneous untangling and smoothing of quadrilateral and hexahedral meshes using an object-oriented framework, *J. Advances in Engineering Software*, 80 (2015) 12–24.
- [21] R. Wang, C. Shen, J. Chen, et al. Automated Block Decomposition of Solid Models Based on Sheet Operations, *J. Procedia Engineering*, 124 (2015) 109–121.
- [22] P. M. Knupp, Algebraic mesh quality metrics for unstructured initial meshes, *J. Finite Elements in Analysis and Design*, 39 (2003) 217–241.